The Disappearance of the Progenitors of Supernovae 1993J and 2003gd

Justyn R. Maund[1,2]* and Stephen J. Smartt[3]

Using images from the Hubble Space Telescope and the Gemini Telescope, we confirmed the disappearance of the progenitors of two type II supernovae (SNe) and evaluated the presence of other stars associated with them. We found that the progenitor of SN 2003gd, an M-supergiant star, is no longer observed at the SN location and determined its intrinsic brightness using image subtraction techniques. The progenitor of SN 1993J, a K-supergiant star, is also no longer present, but its B-supergiant binary companion is still observed. The disappearance of the progenitors confirms that these two supernovae were produced by red supergiants.

Analysis of archival pre-explosion images has helped to identify the progenitors of type II supernovae (SNe), which are thought to result from the explosion of red supergiant stars. In most cases, the progenitors have only been confirmed to be spatially coincident with the SNe, leaving some uncertainty over their correct identification. So far, only one star has been shown to have disappeared after it exploded—the star that exploded as SN 1987A in the Local Group of galaxies (*1*). Seven other stars have been discovered to be spatially coincident with bright, nearby type II SNe (*2*), but none of them have been shown to have disappeared [although recent evidence has suggested the possible disappearance of the progenitor of SN 2005gl (*3*)]. Here, we examine postexplosion images of the sites of two type II SNe to confirm their progenitors' identities.

[1]Dark Cosmology Centre, Niels Bohr Institute, University of Copenhagen, Juliane Maries Vej 30, 2100 Copenhagen Ø, Denmark. [2]Department of Astronomy and Astrophysics, University of California, Santa Cruz, CA 95064, USA. [3]Astrophysics Research Centre, School of Mathematics and Physics, Queen's University Belfast, Belfast BT7 1NN, UK.

*To whom correspondence should be addressed. E-mail: justyn@dark-cosmology.dk

SN 2003gd was discovered in the galaxy M74 and classified as a type II-plateau SN (*4*). The plateau in its light curve and the strong hydrogen P Cygni profiles in its spectrum indicated that it arose from a red supergiant star with a massive hydrogen envelope (*5*). Analysis of pre-explosion images from the Hubble Space Telescope (HST) and Gemini Telescope archives revealed a red supergiant star, with $V = 25.8$, $I = 23.3$ and an initial mass of 8^{+4}_{-2} solar masses ($M_{\odot}$), at the position where the SN occurred (Fig. 1) (*6*, *7*). Five years after the explosion, it is time to verify that this star has disappeared, hoping that the SN remnant has faded to a luminosity below that of its progenitor (as achieved for SN 1987A).

We reimaged the site of SN 2003gd on 6 and 10 September 2008 using the multiobject spectrograph on the Gemini Telescope [GMOS, (*8*)] with the Sloan g', r', and i' filters, under excellent seeing conditions (see Table 1). Using differential astrometry, we matched previous observations of SN 2003gd, acquired with the HST Advanced Camera for Surveys High Resolution Channel (ACS HRC) (*6*), with our GMOS frames to locate the SN position to within 0.031" (Fig. 1). At this position, a single point source is not detected in the i' image, but the SN is still detected significantly at $m_{g'}(AB) = 25.00 \pm 0.04$ and $m_{r'}(AB) = 24.65 \pm 0.05$ [see supporting online material (SOM)]. We compared our i' image with a pre-explosion i' image taken with the GMOS instrument on 14 August 2001, in which the progenitor candidate was detected. After aligning the two images, we scaled the flux levels and the point spread function (PSF) of the postexplosion i'-band image to match those of the pre-explosion image, using the ISIS image subtraction package (*9*, *10*). We then subtracted the scaled post-explosion image from the pre-explosion frame, such that only photometrically variable objects remained (see the SOM for details of the procedure). A point source residual, consistent with a single-star PSF, is present in the pre-explosion image to within 0.023″ of the transformed SN position (Fig. 1) (see SOM). Smartt *et al.* (*6*) found a large offset between the transformed SN position and the object on the pre-explosion frame (0.137 ± 0.071"), leading them to suggest that the object was a blend of the progenitor (Star A) and a nearby star (Star C) (Fig. 1). We find no such offset with our differential astrometric solution, such that the object on the pre-explosion frame is completely consistent with a single star located at the position of Star A. All other single nonvariable stellar objects were cleanly subtracted from the pre-explosion image, with only minor residuals remaining for obviously extended features such as resolved clusters. Hence, the point source visible in the subtracted frame is the i'-band flux from the progenitor, which has now disappeared. There clearly is a faint, extended background feature in the post-explosion image, but this is inconsistent with a single PSF. By conducting forced photometry at the SN position and by adding artificial stars to our postexplosion i' image and attempting to recover them using the ISIS package, we conserv-

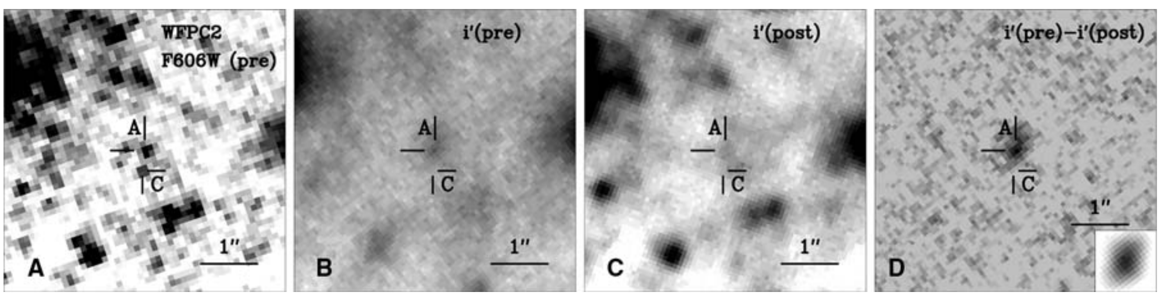

Fig. 1. Pre- and post-explosion images of the site of SN 2003gd taken with the HST WFPC2 and Gemini GMOS instruments (see Table 1 for details). (**A**) Pre-explosion WFPC2 F606W image, with the previously identified progenitor object marked as Star A and a nearby star labeled Star C. (**B**) Pre-explosion Gemini GMOS i' band image, with spatial resolution 0.57'', in which the progenitor is detected. (**C**) Postexplosion Gemini GMOS i' band image where a single point source is not detected at the transformed position of SN 2003gd, with a limit on any remaining SN flux of $m_{i'}(AB) > 26.3$. The image has a spatial resolution of 0.36'', and no point source is detected at the position of Star C, which suggests a negligible contribution in the i'-band from that star. (**D**) Pre-explosion image with the flux/PSF-scaled postexplosion image subtracted. The residual object at the position of SN 2003gd is the progenitor, with any contaminating flux from nearby stars subtracted. The object at the SN location, marked as Star A, is consistent with single-star PSF ($\chi^2 = 0.9$) and has a Johnson I magnitude of 23.14 ± 0.08 [$m_{i'}(AB) = 24.25 \pm 0.04$]. In the bottom right corner, a model single-star PSF is shown. It was determined by ISIS and is consistent with the source detected in this subtraction image.

atively estimate that the upper brightness limit for a single point source is $m_i(AB) > 26.3$ at the SN location. This corresponds to a magnitude difference between the pre- and postexplosion i' images of $\Delta m_{i'} > 2$. The absence of an obvious point source in the postexplosion image, which is within 2 magnitudes of the detected progenitor, further confirms that the star has disappeared.

We transformed the pre-explosion i' band photometry to the Johnson system by bootstrapping the photometry with Wide-Field Camera images from the Isaac Newton Telescope and the M74 standard star sequence used for monitoring both SN 2003gd and SN 2002ap (*11*). These data imply that the progenitor star had a final Johnson I band magnitude of 23.14 ± 0.08, tightening earlier constraints (*6*). This is 0.2 magnitudes brighter than previously reported, due to our determination that Star C contributed negligible i' flux.

Using the HSTphot package (*12*), we analyzed pre-explosion HST Wide-Field Planetary Camera 2 WFPC2 images taken with the F606W filter, which is close to the V-band filter. We used the I-band magnitude determined above to solve the color-transformation equations that convert the F606W instrumental magnitude to the Johnson system and found that the progenitor has a Johnson V magnitude of 25.72 ± 0.09. Correcting for a reddening of $E(B - V) = 0.14 \pm 0.06$, which was determined from photometry of SN 2003gd (*5*), implies an intrinsic color of $(V - I)_0 = 2.41 \pm 0.14$. This is consistent with the progenitor being an M0 to M2 red supergiant star (*13*) but disfavors warmer K-supergiant stars. Applying the appropriate bolometric correction for this range of allowed red supergiants, and correcting for a distance of 9.3 ± 1.8 Mpc to M74 (*5*), yields a luminosity of $\log(L/L_\odot) = 4.29 \pm 0.2$, with an effective temperature of $\log T_{\mathrm{eff}} = 3.54 \pm 0.02$. Comparison with the end points of stellar evolution models shows that this luminosity and temperature region of the Hertzprung-Russell diagram constrains the progenitor to have had initial mass of $7^{+6}_{-1}\ M_\odot$ (*2*).

At the epoch of 6 September 2008 (~2000 days after explosion), the SN is still visible in the wavelength range corresponding to the F622W and Sloan r' filters (see table S7). This is due to the presence of considerable $H\alpha$ emission in the band-passes of these filters, typical of type II SNe at late times (*5*, *14*). The fact that the SN is bright in the late-time F622W observations precludes the use of image subtraction techniques to determine the true progenitor brightness in the pre-explosion WFPC2 F606W image. We need to wait longer until the $H\alpha$ flux fades well below the magnitude of the progenitor star detected in the F606W filter.

One could argue that the star identified as the progenitor was a neighboring star that is now obscured by dust formation in the foreground SN remnant. However, the internal extinction in the SN 2003gd remnant, due to newly formed dust, was estimated to be $A_R < 1.48$ (*15*) or $A_{i'} < 1.22$ (*16*) at 678 days. Using this as the maximum value of the extinction across the SN remnant at the epoch of our GMOS images (assuming no further dust formation), this amount of extinction is insufficient to cause $\Delta m_{i'}$ measured by us. This implies that the object we have identified as the progenitor is not simply obscured by dust in the intervening SN remnant and has actually disappeared.

The progenitor of the hydrogen-bearing (type IIb) SN 1993J was identified as a K-supergiant star, with excess flux at ultraviolet (UV) wavelengths, possibly because of a binary companion or nearby stars (*17*). The model for this binary system was of a 15 $M_\odot$ progenitor star, with a binary companion of slightly lower mass (*18*–*20*). Because the progenitor star evolved faster, it underwent mass transfer onto the binary companion, which removed a substantial amount of its hydrogen envelope, causing a shift to the bluer K spectral type [rather than the canonical M spectral type (*2*)]. The binary companion grew to 22 $M_\odot$ and became the source of the excess UV flux. A later study, using high-resolution HST images, found that some of the UV excess could be explained by nearby previously unresolved stars but that a UV excess still remained unaccounted for (*21*). The binary progenitor scenario was confirmed when spectral features of a massive blue supergiant were detected in late-time spectroscopy (*22*).

The site of SN 1993J was imaged several times over the 2 to 13 years after explosion with the HST WFPC2 ACS HRC and Wide-Field Channels (WFC) (see SOM for full list of dates). By the epoch of the 2004 observation, the red portion of the SN spectral energy distribution (SED) had faded below the level of the SED of

Table 1. Pre- and postexplosion observations of the site of SN 2003gd (*, pixel scale).

Telescope/instrument	Date	Program	Filter	Exposure time (s)	Seeing (")
Gemini GMOS	14 August 2001	GN-2001B-SV-102	i'	480	0.57
HST/WFPC2	25/28 August 2002	GO-9676	F606W	2100	0.1*
HST/ACS/HRC	01 August 2003	GO-9733	F814W	1350	0.025*
Gemini GMOS	10 September 2008	GN-2008B-Q-67	g'	4050	0.53
Gemini GMOS	06 September 2008	GN-2008B-Q-67	r'	1590	0.42
Gemini GMOS	06 September 2008	GN-2008B-Q-67	i'	3180	0.36

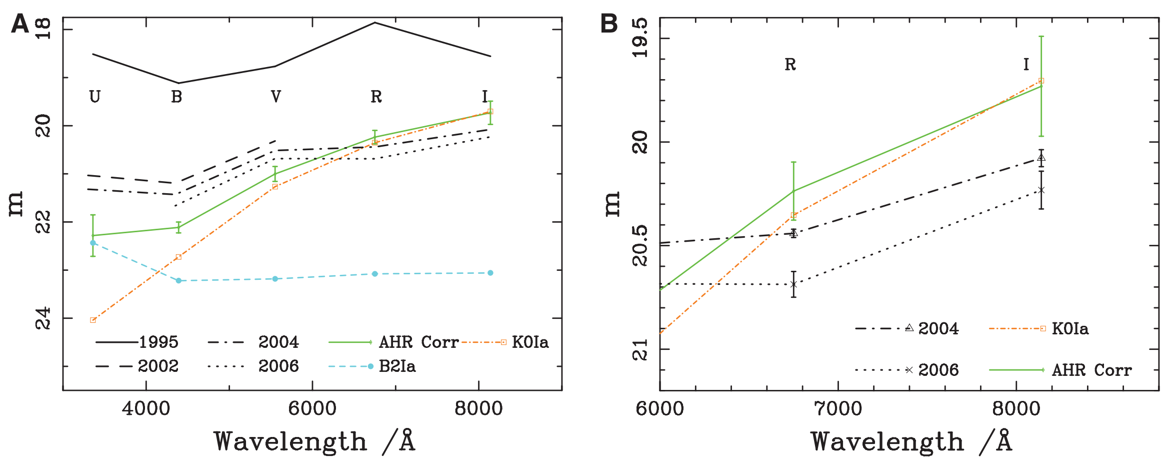

Fig. 2. The SED of the progenitor binary system of SN 1993J. The SED (AHR Corr) (*17*) has been corrected for the excess flux contribution from four nearby stars, unresolved in the low-resolution ground-based pre-explosion imaging, for comparison with photometry of high-resolution HST imaging in which the SN is resolved. (**A**) Overlaid SN 1993J SEDs, measured with HST WFPC2, ACS/HRC, and ACS/WFC, at 31 January 1995, 28 May 2002, 15 July 2004, and 1 and 3 November 2006. The B- and K- supergiant components are the result of a χ^2 fit to the excess corrected pre-explosion photometry (*22*, *26*). (**B**) A zoom in on the R_C and I_C photometric points. Errors on the 2004 and 2006 photometry are calculated from PSF photometry of SN 1993J.

the binary progenitor system (Fig. 2) (see SOM), ruling out the continued presence of the K-supergiant star and, hence, confirming it as the progenitor of SN 1993J. At the current rate of decay of the SN SED, the U- and B-band fluxes will have reached the level of the proposed B-supergiant component by 2012, at which stage it will be possible to directly measure the properties of the remaining companion star.

These results provide observational proof that red supergiant stars are the progenitors of type II SNe, through the disappearance of the previously identified candidate stars of two SNe. Our best estimate for the mass of the progenitor of the type IIP SN 2003gd is 7 $M_{\odot}$ which is at the lower end of the mass range considered theoretically possible to produce core-collapse events. Although the uncertainties (7^{+6}_{-1} $M_{\odot}$) would comfortably allow a large mass for this object, it is interesting that five progenitors of type IIP SNe are found with best estimates at 9 $M_{\odot}$ or below (*2*). This limit is predicted by stellar and SN evolution models (*23*) and is consistent with the upper initial mass limit observed for white dwarfs (*24*). The confirmation of the disappearance of the K-type progenitor star of SN 1993J is further evidence that the binary model previously suggested is valid. It demonstrates the importance of binary interactions for the production of hydrogen-poor SNe (*25*).

References and Notes

1. R. Gilmozzi *et al.*, *Nature* **328**, 318 (1987).
2. S. J. Smartt, J. J. Eldridge, R. M. Crockett, J. R. Maund, *ArXiv*, astro-ph/0809.0403 (2008).
3. A. Gal-Yam, D. Leonard, *Nature* 10.1038/nature07934 (2009).
4. R. Evans, R. H. McNaught, *IAU Circ.* **8150**, 2 (2003).
5. M. A. Hendry *et al.*, *Mon. Not. R. Astron. Soc.* **359**, 906 (2005).
6. S. J. Smartt *et al.*, *Science* **303**, 499 (2004).
7. S. D. Van Dyk, W. Li, A. V. Filippenko, *Publ. Astron. Soc. Pac.* **115**, 1289 (2003).
8. I. M. Hook *et al.*, *Publ. Astron. Soc. Pac.* **116**, 425 (2004).
9. C. Alard, R. H. Lupton, *Astrophys. J.* **503**, 325 (1998).
10. C. Alard, *Astron. Astrophys. Suppl. Ser.* **144**, 363 (2000).
11. A. Henden, *GRB Coord. Network* **1242**, 1 (2002).
12. A. E. Dolphin, *Publ. Astron. Soc. Pac.* **112**, 1383 (2000).
13. J. H. Elias, J. A. Frogel, R. M. Humphreys, *Astrophys. J. Supp. Ser.* **57**, 91 (1985).
14. A. Pastorello *et al., ArXiv*, astro-ph/0901.2075 (2009).
15. B. E. K. Sugerman *et al.*, *Science* **313**, 196 (2006).
16. J. A. Cardelli, G. C. Clayton, J. S. Mathis, *Astrophys. J.* **345**, 245 (1989).
17. G. Aldering, R. M. Humphreys, M. Richmond, *Astron. J.* **107**, 662 (1994).
18. K. Nomoto *et al.*, *Nature* **364**, 507 (1993).
19. P. Podsiadlowski, J. J. L. Hsu, P. C. Joss, R. R. Ross, *Nature* **364**, 509 (1993).
20. S. E. Woosley, R. G. Eastman, T. A. Weaver, P. A. Pinto, *Astrophys. J.* **429**, 300 (1994).
21. S. D. Van Dyk *et al.*, *Publ. Astron. Soc. Pac.* **114**, 1322 (2002).
22. J. R. Maund, S. J. Smartt, R. P. Kudritzki, P. Podsiadlowski, G. F. Gilmore, *Nature* **427**, 129 (2004).
23. J. J. Eldridge, C. A. Tout, *Mon. Not. R. Astron. Soc.* **353**, 87 (2004).
24. K. A. Williams, M. Bolte, D. Koester, *ArXiv*, astro-ph/0811.1577 (2008).
25. P. Podsiadlowski *et al.*, *Astrophys. J.* **612**, 1044 (2004).
26. J. R. Maund, thesis, Institute of Astronomy, Cambridge (2005), www.dark-cosmology.dk/~justyn/research

27. J.R.M. is a Sophie and Tycho Brahe Fellow.

Supporting Online Material

www.sciencemag.org/cgi/content/full/1170198/DC1
SOM Text
Figs. S1 to S4
Tables S1 to S9
References

23 December 2008; accepted 11 March 2009
Published online 19 March 2009;
10.1126/science.1170198
Include this information when citing this paper.

Greatly Increased Toughness of Infiltrated Spider Silk

Seung-Mo Lee,[1]* Eckhard Pippel,[1] Ulrich Gösele,[1] Christian Dresbach,[2] Yong Qin,[1] C. Vinod Chandran,[3] Thomas Bräuniger,[3] Gerd Hause,[4] Mato Knez[1]*

In nature, tiny amounts of inorganic impurities, such as metals, are incorporated in the protein structures of some biomaterials and lead to unusual mechanical properties of those materials. A desire to produce these biomimicking new materials has stimulated materials scientists, and diverse approaches have been attempted. In contrast, research to improve the mechanical properties of biomaterials themselves by direct metal incorporation into inner protein structures has rarely been tried because of the difficulty of developing a method that can infiltrate metals into biomaterials, resulting in a metal-incorporated protein matrix. We demonstrated that metals can be intentionally infiltrated into inner protein structures of biomaterials through multiple pulsed vapor-phase infiltration performed with equipment conventionally used for atomic layer deposition (ALD). We infiltrated zinc (Zn), titanium (Ti), or aluminum (Al), combined with water from corresponding ALD precursors, into spider dragline silks and observed greatly improved toughness of the resulting silks. The presence of the infiltrated metals such as Al or Ti was verified by energy-dispersive x-ray (EDX) and nuclear magnetic resonance spectra measured inside the treated silks. This result of enhanced toughness of spider silk could potentially serve as a model for a more general approach to enhance the strength and toughness of other biomaterials.

In the field of biomaterials research, Bryan and Gibbs suggested that metals such as Cu and Zn, which are incorporated in an inner protein matrix, might play a role in mechanical hardening of the jaws of the marine polychaete worm *Nereis* (*1*, *2*). Many groups have investigated the correlation between the presence of some metal elements, such as Zn, Mn, Ca, or Cu, accumulated in the cuticles of insects or other organisms (in body parts such as mandibles, stingers, claws, and ovipositors) and their enhanced mechanical properties (particularly stiffness and hardness) (*3*–*15*). We demonstrated that inorganic impurities such as Zn, Ti, and Al can be inserted into biomaterials by the multiple pulsed vapor-phase infiltration (MPI) process (Fig. 1), performed with equipment conventionally used for atomic layer deposition (ALD).

For testing, we selected spider dragline silk from major ampullate silk glands, which outperforms almost any human-made fiber in its combination of tensile strength (σ) and extensibility (ε) (its so-called extreme toughness, $\int\sigma d\varepsilon$) (*16*, *17*). A number of scientists have claimed a strong relation between Zn accumulated in insect cuticles, such as the mandibles of the leaf-cutter ant (*3*, *6*), locust (*9*), and marine polychaete worm *Nereis* (*10*), and the enhanced hardness and stiffness of these biomaterials. Broomell *et al.* showed that a metal ion (Zn^{2+}) plays a critical role in the mechanical properties of *Nereis* jaws, by nanoindentation measurements performed before and after Zn chelation (*12*). Therefore, we initially alternately exposed the dragline silk to the vapor of diethylzinc (DEZ) [$Zn(C_2H_5)_2$] and water (H_2O) (table S1) (*18*) in an ALD reactor and observed a considerable increase of both σ_{max} (the maximum stress) and E_{ini} (the initial Young's modulus) as compared to those of the untreated native (N) dragline spider silk (SS) (SS/N), which had mechanical properties close to those reported in the literature for the *Araneus* spider's dragline silk [σ_{max} (SS/N) ≈ 1.1 GPa and E_{ini} (SS/N) ≈ 10 GPa)] (*19*) (fig. S2 and table S2). We subsequently observed that dragline silks exposed to $Al(CH_3)_3$ [trimethylaluminum (TMA)]/H_2O or $Ti(OCH(CH_3)_2)_4$ [titanium(IV) isopropoxide (TIP)]/H_2O pulse pairs showed considerably larger improvements in toughness than silks exposed to the DEZ/H_2O pair.

An ALD process conventionally leads to thin deposited layers of metal oxide on a fiber (Fig. 1). Therefore, the question arises whether the increased σ_{max} could be considered a result of

[1]Max Planck Institute of Microstructure Physics, Weinberg 2, D-06120 Halle, Germany. [2]Fraunhofer Institute for Mechanics of Materials, Walter-Hülse-Straße 1, D-06120 Halle, Germany. [3]Institute of Physics–Nuclear Magnetic Resonance Group, Martin-Luther-University Halle-Wittenberg, Friedemann-Bach-Platz 6, D-06108 Halle, Germany. [4]Microscopy Unit Biocenter, Martin-Luther-University Halle-Wittenberg, Weinbergweg 22, D-06120 Halle, Germany.

*To whom correspondence should be addressed. E-mail: smlee@mpi-halle.de (S.-M.L.); mknez@mpi-halle.de (M.K.)

Science

The Disappearance of the Progenitors of Supernovae 1993J and 2003gd

Justyn R. Maund and Stephen J. Smartt

Science **324** (5926), 486-488.
DOI: 10.1126/science.1170198originally published online March 19, 2009

Disappearing Stars
One way to identify and study the stars that have exploded as supernovae is to look for stars that are spatially coincident with the supernovae in pre-explosion images. The only way to be sure of their identifications is to wait for the light from the supernovae to fade and check that the stars have vanished from the sky. **Maund and Smartt** (p. 486, published online 19 March), using the Hubble Space Telescope and the Gemini telescope, have now shown that the red supergiant stars that have been found in pre-explosion images of SN 2003gd and SN 1993J are no longer seen in recent images of the supernovae sites. Their absence confirms that they were the supernovae's true progenitors.